This is a repository copy of *The Impact of Cracks on Photovoltaic Power Performance*.

Article:

The Impact of Cracks on Photovoltaic Power Performance

Abstract

This paper presents a statistical approach for identifying the significant impact of cracks on the output power performance for photovoltaic (PV) modules. There are a few data statistical analysis for investigating the impact of cracks in PV modules in real-time long-term field data measurements. Therefore, this paper will demonstrate a statistical analysis approach which uses T-test and F-test for identifying whether the crack has a significant or non-significant impact on the total amount of power generated by the PV modules. Electroluminescence (EL) method is used for scanning possible faults in the examined PV modules. However, Virtual Instrumentation (VI) LabVIEW software is used to simulate the theoretical I-V and P-V curves. The approach classified only 60% of cracks that has a significant impact on the total amount of power generated by PV modules.

Keywords: Photovoltaic (PV) Module Performance; Solar cell cracks; Statistical Approach; Electroluminescence (EL); Surface Analysis

1. Introduction

Cell cracks appear in the photovoltaic (PV) panels during their transportation from the factory to the place of installation. Also, some climate proceedings such as snow loads, strong winds and hailstorms might create some major cracks on the PV modules surface [1-3]. These cracks may lead to disconnection of cells parts and, therefore, to a loss in the total power generated by the PV modules [4].

There are several types of cracks that might occur in PV modules: diagonal cracks, parallel to busbars crack, perpendicular to busbars crack and multiple directions crack. Diagonal Cracks and multiple directions cracks always show a significant reduction in the PV output power [5].

Moreover, the PV industry has reacted to the in-line non-destructive cracks by developing new techniques of crack detection such as resonance ultrasonic vibration (RUV) for screening PV cells with pre-existing cracks [6]. This helped to reduce cell cracking due to defective wafers, but, it does not mitigate the cracks generated during the manufacturing process of PV modules.

When cracks appear in a solar cell, the parts separated from the cell might not be totally disconnected, but the series resistance across the crack varies as a function of the distance between the cell parts and the number of cycles for which module is deformed [7]. However, when a cell part is fully isolated, the current decrease is proportional to the disconnected area [8, 9].

Collecting the data from damaged PV modules using installed systems is a challenging task. Electroluminescence (EL) imaging method is used to scan the surface of the PV modules, the light output increases with the local voltage so that regions with poor contact show up as dark spots [10, 11]. The thermography technique is simpler to implement, but the accuracy of the image is lower than with the EL technique, and does not allow the estimation of the area (in mm^2) that is broken in the solar cells [12, 13]. Therefore, in this paper we have used EL imaging method which can be illustrated and discussed briefly in the following articles [14-16].

As proposed in [17] the performance of PV systems can be monitored using virtual instrumentation software such as LabVIEW. Also MATLAB software allows users to create tools to model, monitor and estimate the performance of photovoltaic systems. The simulation tool is important to compare the output measured data from PV module with its own theoretical performance [18].

There are a few statistical analysis tools that have been deployed in PV applications. The common used tool is the normal standard deviation limits ($\pm$ 1 SD or $\pm$ 3 SD) technique [19]. However, [20] used a statistical local distribution analysis in identifying the type of cracks in a PV modules. To the best of our knowledge, few of the reviewed articles have used a real-time long-term statistical analysis approach for PV cracked modules under real-time operational process. Therefore, the main contribution of this work can be illustrated as the following:

- Development of a novel statistical analysis approach that can be used to identify the significant effect of cracks on the output power performance for PV modules under various environmental field data measurements.
- Proving that not all cracks has a significant impact on the PV output power performance.

This paper is organized as follows: Section 2 describes the methodology used which contains the data acquisition, PV modules cracks and the statistical analysis approach, while Section 3 lists the output results of the entire work. The discussion is presented in section 4. Finally, Sections 5 and 6 describes the conclusion and the acknowledgment respectively.

2. Methodology

2.1. Data acquisition

In this work, we used a statistical study of broken cells showing different crack types. Several test measurements are carried out on two different PV plants at the University of Huddersfield, United Kingdom. The first system consists of 10 polycrystalline PV modules with an optimum power 220Wp. However, the second system consists of 35 polycrystalline with 130Wp each. Both systems are shown in Fig. 1.

As presented in Fig. 1(A) and Fig 1(B), there are two examined PV systems with total amount of PV modules equal to 45. To establish the connection for each PV module separately, a controlling unit is designed to allow the user to connect any PV module to a FLEXmax 80 MPPT. In order to facilitate a real-time monitoring for each PV module, therefore, Vantage Pro monitoring unit is used to receive the Global solar irradiance measured by Davis weather station which includes pyranometer. Hub 4 communication manager is used to facilitate acquisition of modules temperature using Davis external temperature sensor, and the electrical data for each photovoltaic

76 module. LabVIEW software is used to implement the data logging and monitoring functions of
77 the examined PV modules.

78 Fig. 1(C) shows the data acquisition system. Furthermore, Table I illustrates both electrical
79 characteristics of the solar modules that are used in this work. The standard test condition (STC)
80 for all examined solar panels are: Solar Irradiance = 1000 W/m^2; Module Temperature = 25 °C.

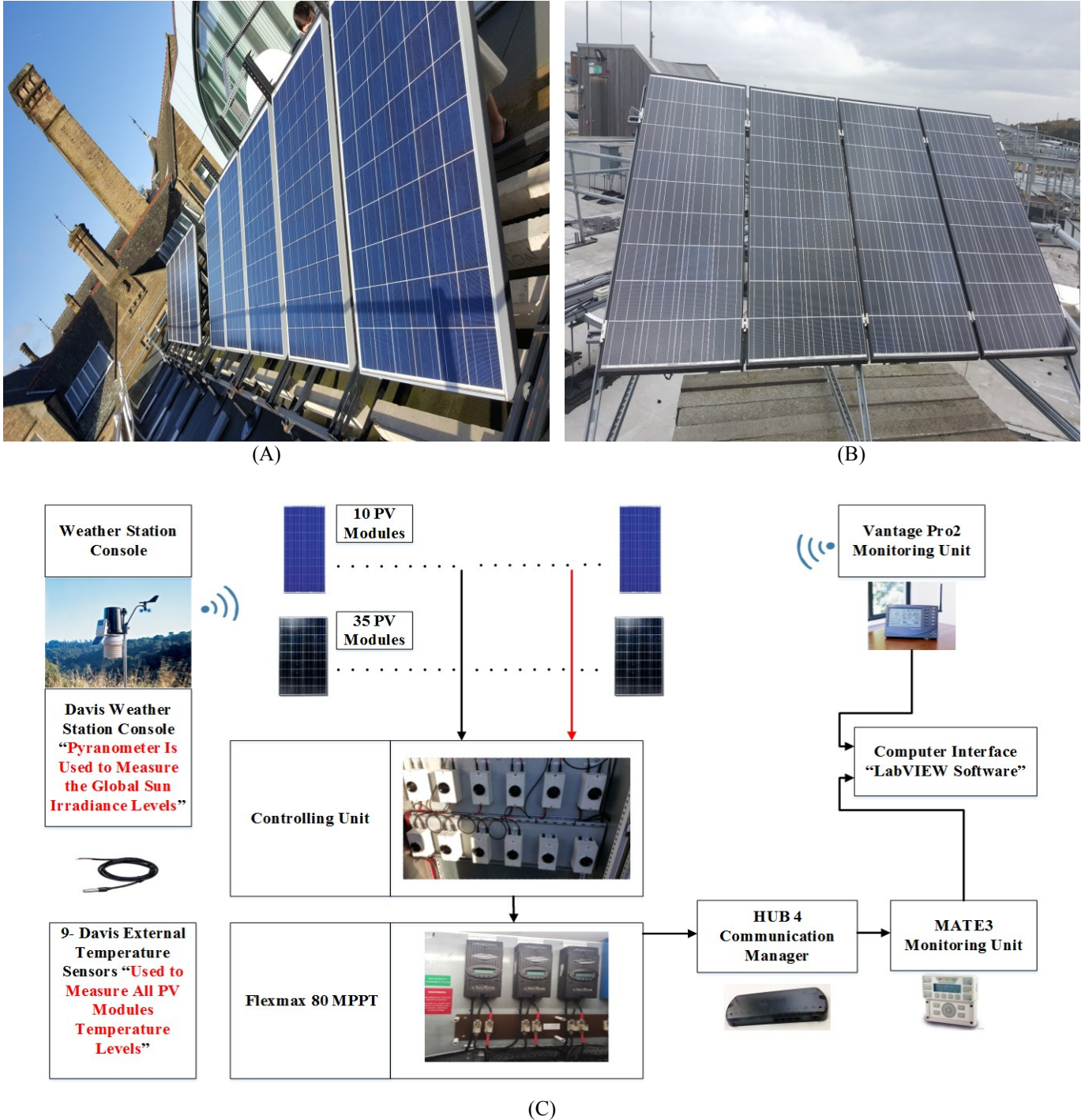(A)   (B)

(C)

Fig. 1. (A) 10 PV Modules (SMT 6 (60) P) with 220W Output Peak Power; (B) 35 PV Modules (KC130 GHT-2) with 130W Output Peak Power; (C) Monitoring the Examined PV System Using LabVIEW Software

TABLE I
ELECTRICAL CHARACTERISTICS FOR BOTH PV SYSTEMS MODULES

Solar Panel Electrical Characteristics	1ST System: PV Module, SMT 6 (60) P	2nd System: PV Module, KC130 GHT-2
Peak Power	220 W	130
Voltage at Maximum Power Point (V_{mp})	28.7 V	17.6
Current at Maximum Power Point (I_{mp})	7.67 A	7.39
Open Circuit Voltage (V_{OC})	36.74 V	21.9
Short Circuit Current (I_{sc})	8.24 A	8.02
Number of Cells Connected in Series	60	36
Number of Cells Connected in Parallel	1	1
PV System Tilt Angle and Azimuth Angle (North-South)	42°, 185°	42°, 180°
Davis Pyranometer Sensor Tilt Angle and Azimuth Angles (North-South)	42°, 185°	42°, 180°

2.2. Electroluminescence setup and PV modules cracks

The electroluminescence system developed is presented in Fig. 2(A). The system is comprised of a light-tight black-box where housed inside is a digital camera and a sample holder. The digital camera is equipped with a standard F-mount 18–55 mm lens. To allow for detection in the near infrared, the IR filter was removed and replaced with a full spectrum window of equal optical path length. In our setup a Nikon D40 was used, but in principle any digital camera with similar grade CCD or CMOS sensor and where the IR filter can be removed would serve the purpose. The bias was applied and the resultant current and the voltage are measured by a voltage and current sensors which are wirelessly connected to the personal computer (PC). The purpose of the PC is to get the electroluminescence image of the solar module and predicting the theoretical output power performance of the PV module.

In order to reduce the noise and increase the accuracy, all EL images are processed by removing background noise and erroneous pixels. Firstly, background image has been captured under the same conditions as the EL images but without forward biasing the cell. This background image is subtracted from each EL image in order to reduce the image noise level. The images are cropped to the appropriate size and in the case of high resolution imaging system the captured cell images are compiled together to form an image of the entire module. Additionally, to increase the accuracy and the vision of the EL image, each PV module cell is captured separately.

In order to determine the cracks location, type and size; reflex camera has been used for imaging possible cracks in each PV module. As explained previously in the introduction, EL imaging technique is used worldwide and it has been demonstrated by many researchers [14-16]. Broken cells are sorted according to the type of crack, Fig. 2 shows all examined crack types which are classified as the following:

A. Diagonal crack ($+45^0$)
B. Diagonal crack ($- 45^0$)
C. Parallel to busbars crack
D. Perpendicular to busbars crack
E. Multiple directions crack
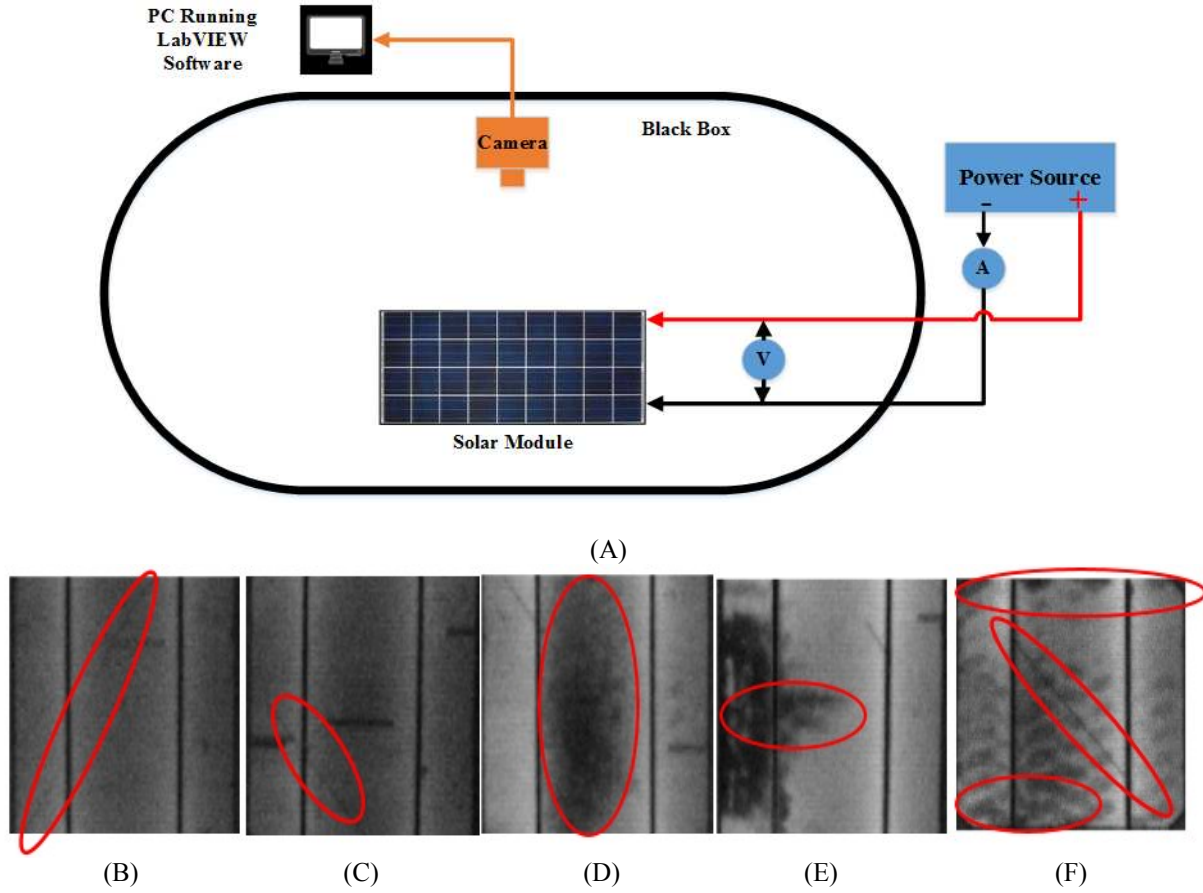
4

(A)

| (B) | (C) | (D) | (E) | (F) |

Fig. 2. El Experimental Setup and Examined Crack Types. (A) Electroluminescence experimental setup; (B) Diagonal Crack $(+45^0)$; (C) Diagonal Crack (-45^0); (D) Parallel to Busbars Crack; (E) Perpendicular to Busbars Crack; (F) Multiple Directions Crack

2.3. Theoretical output power modelling

The DC-Side for all examined PV modules is modelled using 5-parameters model. The voltage and the current characteristics of the PV module can be obtained using the single diode model [21] as the following:

$$I = I_{ph} - I_o \left(e^{\frac{V+IR_S}{nsV_t}} - 1 \right) - (\frac{V+IR_S}{R_{sh}}) \tag{1}$$

Where I_{ph} is the photo-generated current at STC , I_o is the dark saturation current at STC, R_s is the module series resistance, R_{sh} is the panel parallel resistance, ns is the number of series cells in the PV module and V_t is the thermal voltage and it can be defined based on:

$$V_t = \frac{A K T}{q} \tag{2}$$

Where A the diode ideality factor, k is Boltzmann's constant and q is the charge of the electron.

The five parameters model are determined by solving the transcendental equation (1) using Newton-Raphson algorithm. Based only on the datasheet of the available parameters shown previously in Table I. The power produced by PV module in watts can be easily calculated along with the current (I) and voltage (V) that is generated by equation (1), therefore, $P_{theoretical} = IV$.

2.4. Statistical analysis approach

After examining all PV modules which have cracks, a real time simulation can be processed. A statistical analysis approach is used to determine whether the PV crack has a significant impact on the total generated output power performance or not. Two statistical methods are used, T-test and F-test. The first method (T-test) is used to compare the simulated theoretical power with the measured PV output power. T-test can be evaluated using (3) where $\overline{x}$ is the mean of the samples, μ is the population mean, n is the sample size and SD is the standard deviation of the entire data.

In this work, we have used a confidence interval for all measured samples equal to 99%. Statistically speaking, the crack does not have a significant impact on the output power performance if the t-test value is significant, which means that the t-test value is less than or equal to 2.58 as shown in Table II.

If the t-test value is not significant, another statistical method/layer is used to compare the output measured power from the cracked PV module with a PV module that has 0% of cracks. This layer is used to confirm that the output generated power of the cracked PV module has a significant impact (Real Damage) on the total generated output power performance of the examined photovoltaic module. In section 4 (results section), most of the inspected results indicates that if the T-test value is significant, F-test value is also significant. The overall statistical approach can be explained in Fig. 3 and F-test can be evaluated using (4). The explained variance is calculated using between groups mean square value, the unexplained variance is calculated using within groups mean square value [22].

Table III, illustrates the expected output results from F-test using 99% (P=0.01) confidence interval. In this work, an infinite number of samples (Total measured samples > 120) is used to determine whether the F-test value is significant (F-test $\leq$ 6.635) or not significant (F-test > 6.635).

$$t = \frac{(\overline{x} - \mu)\sqrt{n}}{SD} \tag{3}$$

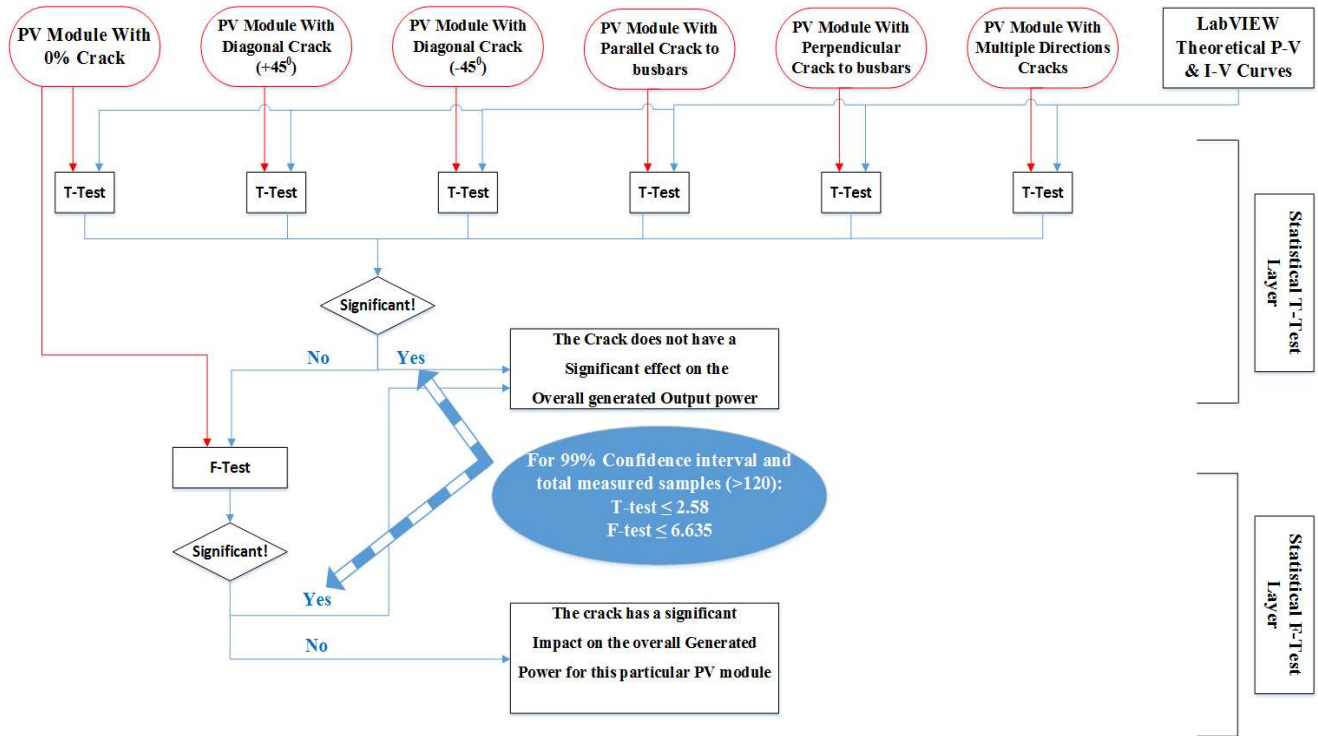$$F = \frac{Explained\ Variance}{Unexplained\ Variance} \tag{4}$$

Fig. 3. Statistical Approach Used to Identify Whether the Crack Type has a Significant Impact on the Output Power Performance of a Photovoltaic Module

TABLE II
STATISTICAL T-TEST CONFIDENCE INTERVAL [22]

Value of t for Confidence Interval of Critical Value |t| for P Values of Number of Degrees of Freedom	90 % (P=0.1)	95% (P=0.05)	99% (P=0.01)
1	6.31	12.71	63.66
20	1.72	2.09	2.85
50	1.68	2.01	2.68
∞	1.64	1.96	2.58

TABLE III
STATISTICAL F-TEST CRITICAL VALUES FOR 99% CONFIDENCE INTERVAL (P=0.01) [22]

Degree of Freedom (Measured Samples)	Output F-test For a Significant Results
1	4052.181
120	4.787
∞	6.635

148

7

3. Results

3.1. Cracks distribution

As described previously, the statistic micro cracks location, type and size was established by taking EL images of 45 PV modules. The EL images are taken with a reflex camera [23]. From the captured pictures, the number of cracked cells in each module is counted as shown in Fig. 4.

Broken cells are sorted according to the type of crack they show and the classification already presented in Fig. 2. The probability for a cell to be cracked and the crack-type distribution are presented in Fig .4. Only 15.556% of the total PV modules have no cracks. However, 84.444% of the PV modules contains at least one type of the crack: diagonal (26.666%), parallel to busbars (20%), perpendicular to busbars (8.888%) or multiple directions crack (28.888%).

According to the statistical approach explained previously in Fig. 3, T-test and F-test methods are significant based on a threshold values. Therefore, we have divided all crack-types into two main categories:

- Short: Crack effects one solar cell in a PV module

- Long: Crack effects two or more solar cell in a PV module

Furthermore, fitted line regression is used for the entire measured PV crack-type data. A fitted regression represents a mathematical regression equation for the PV measured data. We have selected the fitted regression lines to illustrate the relationship between a predictor variable (Measured PV Power) and a response variable (Irradiance Level) and to evaluate whether the model fits the data. If the measured PV power data is very close to the fitted line regression model, therefore, there is a significant relationship between the predictor with the response variable.
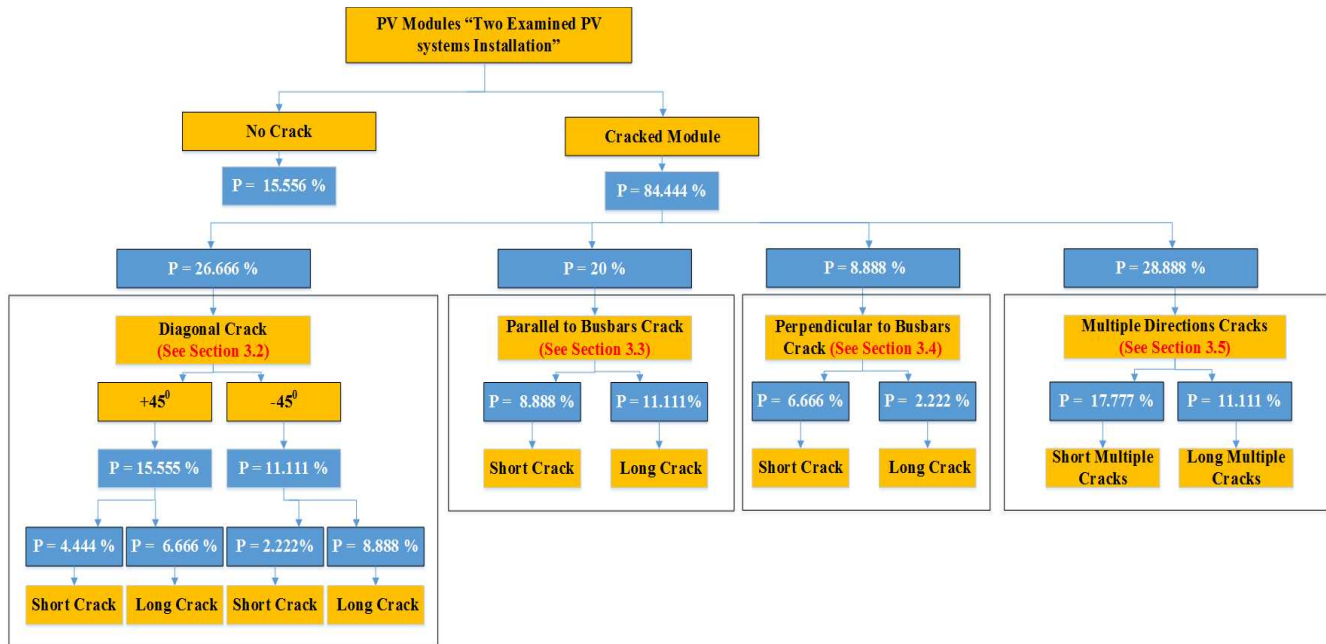

Fig. 4. Crack Types Probability Distribution among Both Examined PV Systems (45 PV Modules)

3.2. Diagonal cracks

Diagonal cracks can be classified into two different categories: $+45^0$ and -45^0 as shown in Fig. 2(A) and 2(B) respectively. The measured data which has been carried out from both diagonal crack categories indicate that there is a huge similarity in the measured output power performance for all examined PV modules. Therefore, we have classified both categories in one crack type. This result is different from the results explained in [7, 8] because all the measured data in our experiments were taken from a real-time long-term environmental measurements instead of laboratory climate conditions.

Using the statistical approach, the T-test values for all examined diagonal crack PV modules (12 PV modules) are shown in Table IV. Since the T-test value for a diagonal crack effects 1 or 2 solar cells is less than 99% of the confidence interval threshold (2.58), the output power performance for the PV module is statistically not significant: No evidence for a real damage in the PV module. The F-test for a diagonal crack effects 1 or 2 solar cells is equal to 4.55 and 5.67 respectively. The mathematical expressions for the fitted line regression are illustrated in Table IV.

A real-time long-term measured data for a full day is carried out to estimate the output power performance for a diagonal crack which effects 1 and 5 solar cells are presented in Fig. 5(A). The theoretical simulated output power which is calculated using LabVIEW software has a standard deviation equals to 61.46 which is very close to the standard deviation for a diagonal crack which effects 1 solar cell (SD=61.38). However, a diagonal crack effects 5 solar cells has a huge reduction in the output power performance of the PV module where the standard deviation is equal to 60.99. Finally, the measured output power of the PV module matches the theoretical output power, therefore, the theoretical power in Fig. 5(A) cannot be seen, this results is also occurring in Fig. 6(A), Fig. 7(A) and Fig. 8(A).

Fig. 5(B) describes the output power efficiency for the examined diagonal cracks effects 1, 2, 3, 4 and 5 solar cells. Between 0.35 - 0.44% reduction of power estimated for a diagonal crack effects 1 solar cell. However, the estimated reduction of power for a diagonal crack effects 5 solar cells is between 2.97 - 5.37%. The output power efficiency can be estimated using (5).

Table IV

Diagonal Cracks Performance Indicators

| Diagonal Crack	Number of Effected Solar Cells	Approximate Area Broken (mm)	T-test Value	Significant/Not Significant Effect on the PV Power Performance	Fitted Line Regression Equation
Short $+45^0$ OR Short -45^0	1	1 mm^2 – 83 mm^2	0.40 - 0.66	**Not Significant**	$P_{TH} = 0.1424 + 1.001\,P_{Meas}$
Long $+45^0$ OR Long -45^0	2	85.85 mm^2 – 169.7 mm^2	1.22 – 1.86	**Not Significant**	$P_{TH} = 0.2875 + 1.003\,P_{Meas}$
	3	172.7 mm^2 - 256.6 mm^2	2.51 - 2.71	Significant	$P_{TH} = 0.5125 + 1.006\,P_{Meas}$
	4	257. 5 mm^2 - 344.4 mm^2	2.65 – 2.70	Significant	$P_{TH} = 0.7034 + 1.008\,P_{Meas}$
	5	345.1 mm^2 – 424.3 mm^2	3.12 – 3.35	Significant	$P_{TH} = 1.151 + 1.013\,P_{Meas}$
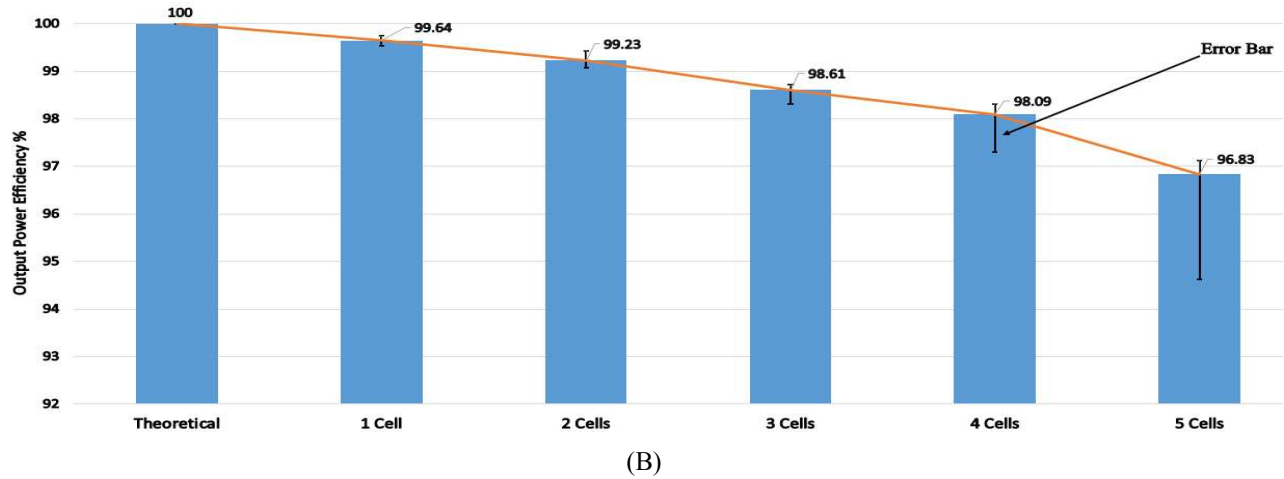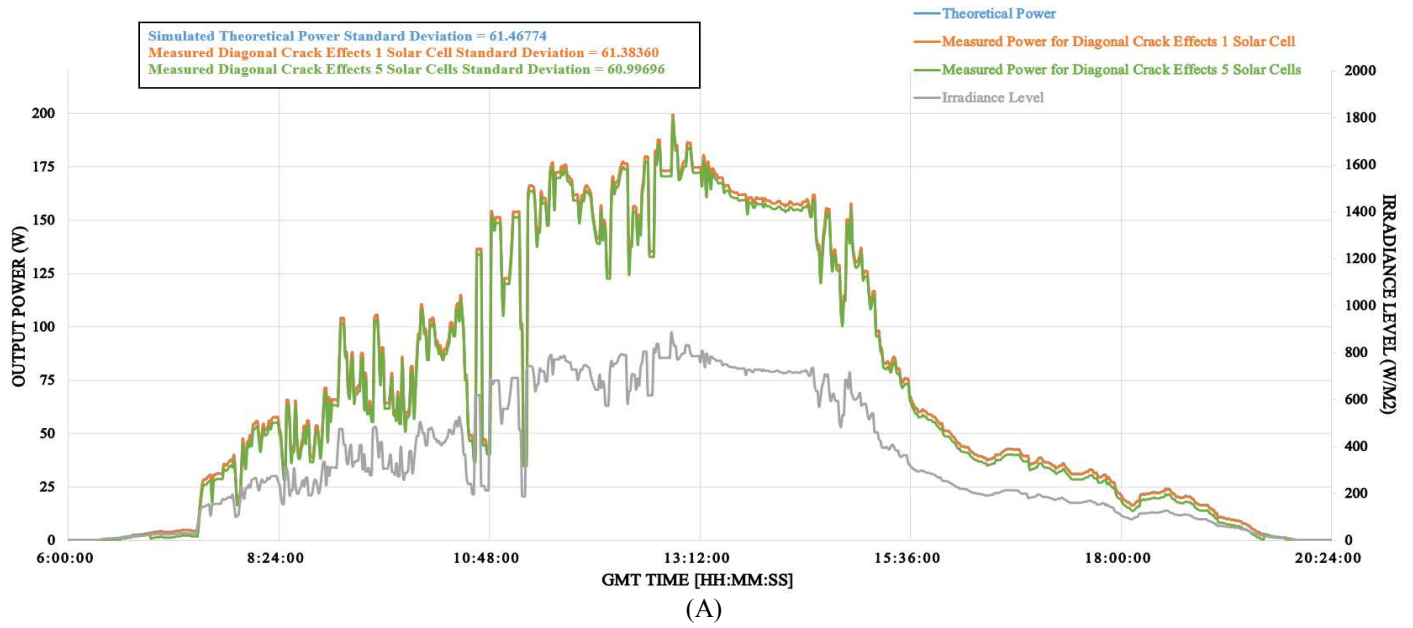
Fig. 5.   (A) Real-Time Long-Term Measured Data for a Diagonal Crack Effects 1 and 5 Solar Cells; (B) Output Power Efficiency for a Diagonal Cracks Which Effects 1, 2, 3, 4 and 5 PV Solar Cells

3.3. Parallel to busbars cracks

As explained previously in Fig. 5, parallel to the busbars cracks has a percentage of occurrence 20% (9 PV modules out of 45 examined PV modules) and they are listed as the following:

- 8.888% (4 PV modules): Short Crack Effect
- 11.111% (5 PV modules): Long Crack Effect

Not all parallel to busbars cracks has a significant impact/reduction on the output power performance of the PV module. As shown in Table V, parallel to busbars cracks effects 1 solar cell statistically indicates that there is no real damage in the PV module, the result is confirmed by the T-test value which is less than the threshold value 2.58. Moreover, when a parallel to busbars crack effects 2 solar cells with approximate broken area less than $82mm^2$ have no significant effect on the amount of power generated by the PV module. Additionally, Table V illustrates various

10

208　mathematical equations for the measured fitted line regression which describes the relationship
209　between the theoretical and measured output power.

210　Fig. 6(A) presents real-time measured data for a parallel to busbars crack effects 1 and 4 solar
211　cells. The standard deviation for the theoretical simulated power is 62.01 which is very close to
212　the standard deviation for a parallel to busbars crack effects 1 solar cell (61.8). However, parallel
213　to busbars crack effects 5 solar cells has a huge reduction in the output power performance of the
214　PV module while the standard deviation is equal to 61.09.

215　Fig. 6(B) describes the output power efficiency for the examined parallel to busbars cracks effects
216　1, 2, 3 and 4 solar cells. The reduction of power estimated for a parallel to busbars crack effects 1
217　solar cell is between 0.75% - 0.97%. However, the estimated reduction of power for a parallel to
218　busbars crack effects 3 and 4 solar cells is between 2.39% - 3.0% and 3.67% - 4.55% respectively.
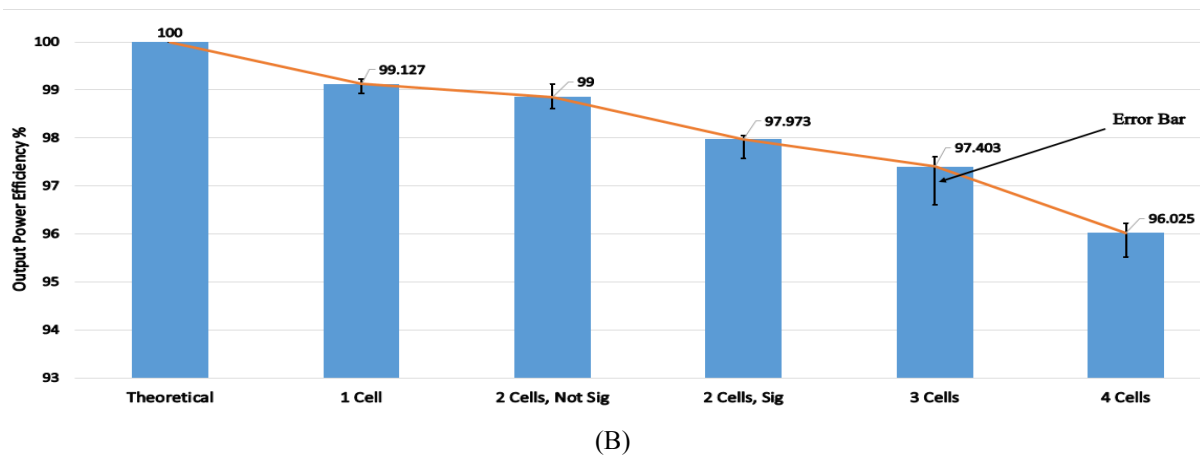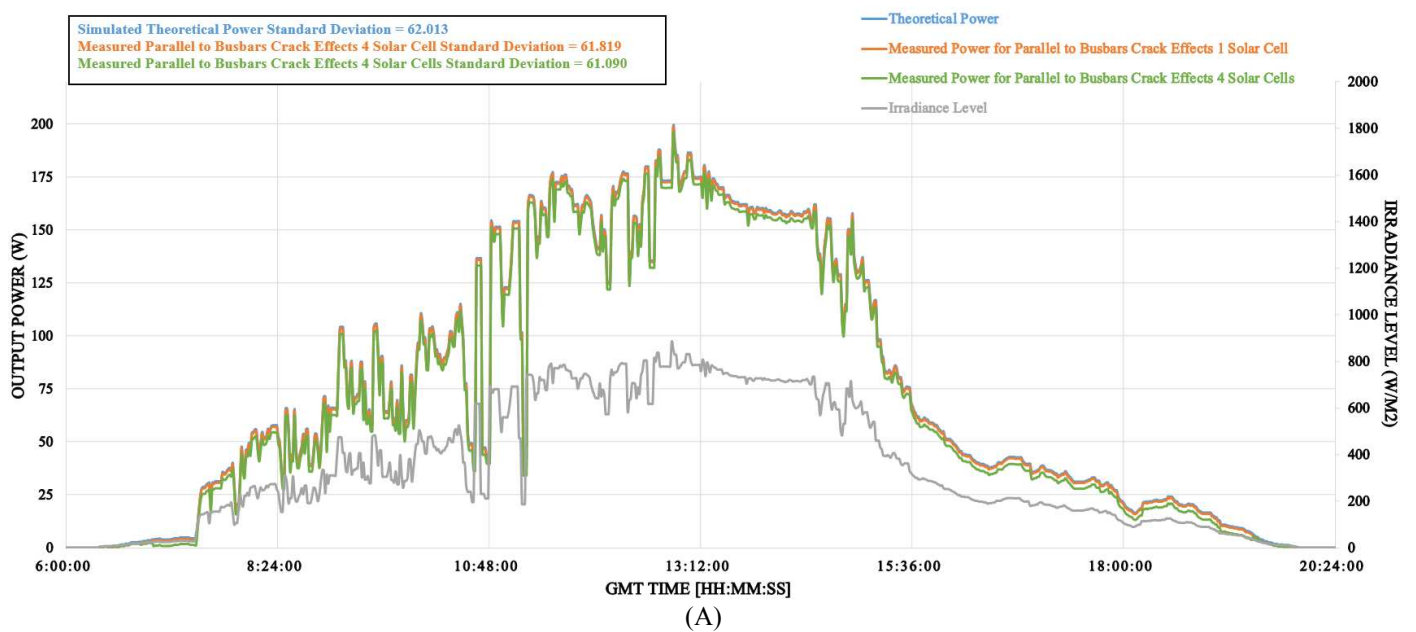

(A)

(B)

Fig. 6.　(A) Real-Time Long-Term Measured Data for a Parallel to Busbars Crack Which Effects 1 and 4 Solar Cells; (B) Output Power Efficiency for Parallel to Busbars Crack Which Effects 1, 2, 3 and 4 PV Solar Cells

$$Efficiency = \frac{Meaured\ Output\ Power}{Theoretical\ Output\ Power} \times 100\% \qquad (5)$$

Table V

Parallel to Busbars Cracks Performance Indicators

Crack Type		Number of Effected Solar Cells	Approximate Area Broken (mm)	T-test Value	Significant/Not Significant Effect on the PV Power Performance	Fitted Line Regression Equation
Parallel To Busbars	Short	1	1 mm^2 – 59.2 mm^2	0.78 – 1.13	**Not Significant**	$P_{TH} = 0.3002 + 1.001\ P_{Meas}$
	Long	2	63 mm^2 – 81 mm^2	1.42 – 1.87	**Not Significant**	$P_{TH} = 0.3990 + 1.004\ P_{Meas}$
			82 mm^2 – 121 mm^2	2.62 – 2.74	Significant	$P_{TH} = 0.6923 + 1.008\ P_{Meas}$
		3	122 mm^2 – 177 mm^2	4.04 – 4.81	Significant	$P_{TH} = 0.9218 + 1.010\ P_{Meas}$
		4	177.3 mm^2 – 239.7 mm^2	4.39 – 5.66	Significant	$P_{TH} = 1.3590 + 1.016\ P_{Meas}$

3.4. Perpendicular to busbars cracks

Perpendicular to busbars cracks usually do not occur in PV modules. In research have distinguished only 4 PV modules from 45 to be classified as a perpendicular to busbars cracks. This result has been verified by many articles such as [7, 8]. Table VI shows all numerical results which are measured from the examined PV modules.

Table VI indicates that a perpendicular to busbars crack effects 1, 2 and 3 busbars statistically has no significant impact on the overall amount of power produced by a PV module. The measured results for a perpendicular to busbars cracks effects 1 and 4 solar cells can be seen in Fig. 7 (A), the difference between the theoretical standard deviation and a perpendicular to busbars cracks which effects 4 solar cells is equal to 1.014. Finally, Fig. 7(b) illustrates the output power efficiency measured for a perpendicular to busbars which effects 1, 2, 3 and 4 solar cells (1-8 Busbars), where the maximum power reduction is estimated for 8 busbars between 4.6 – 4.1%.

Table VI

Perpendicular to Busbars Cracks Performance Indicators

| Crack Type		Number of Effected Solar Cells	Number of Effected Busbars	Approximate Area Broken (mm)	T-test Value	Significant/Not Significant Effect on the PV Power Performance	Fitted Line Regression Equation
Perpendicular To Busbars	Short	1	1	1 mm^2 – 16.2 mm^2	0.65 – 0.82	**Not Significant**	$P_{TH} = 0.0927 + 1.001\ P_{Meas}$
			2	16.3 mm^2 – 60 mm^2	0.92 – 1.31	**Not Significant**	$P_{TH} = 0.1524 + 1.002\ P_{Meas}$
	Long	2	3	61.3 mm^2 – 78.5 mm^2	1.43 – 1.96	**Not Significant**	$P_{TH} = 0.3604 + 1.004\ P_{Meas}$
			4	79.4 mm^2 – 120 mm^2	2.52 – 2.77	Significant	$P_{TH} = 0.4678 + 1.005\ P_{Meas}$
		3	5	120.5 mm^2 – 137.4 mm^2	2.83 – 2.94	Significant	$P_{TH} = 0.7397 + 1.008\ P_{Meas}$
			6	138 mm^2 – 179.8 mm^2	2.79 – 3.11	Significant	$P_{TH} = 0.9265 + 1.010\ P_{Meas}$
		4	7	181.5 mm^2 – 195 mm^2	3.02 – 3.27	Significant	$P_{TH} = 1.0790 + 1.012\ P_{Meas}$
			8	196.2 mm^2 – 240.2 mm^2	3.10 – 3.55	Significant	$P_{TH} = 1.4590 + 1.018\ P_{Meas}$
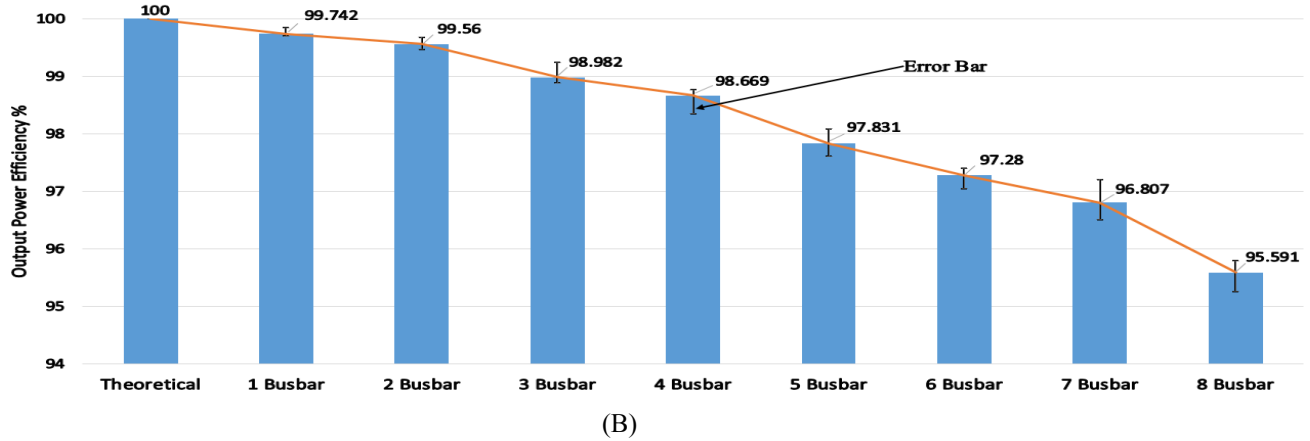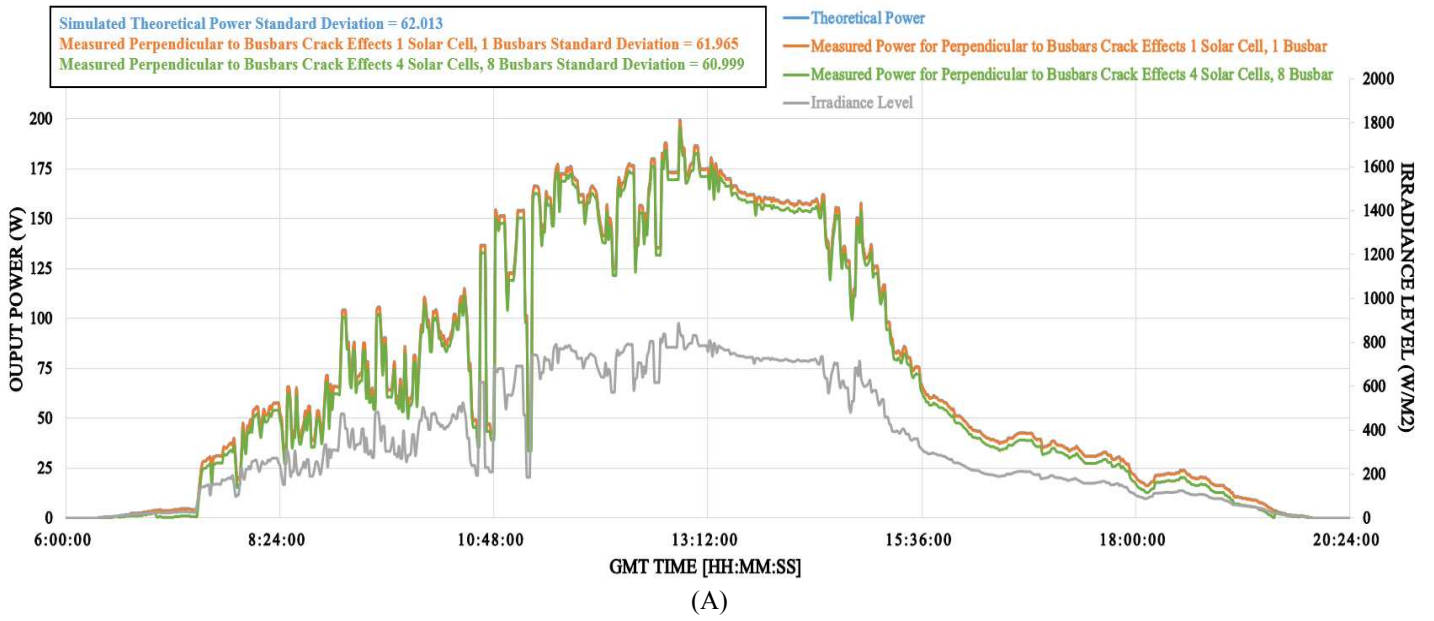
Fig. 7. (A) Real-Time Long-Term Measured Data for a Perpendicular to Busbars Crack Effects 1 and 4 Solar Cells; (B) Output Power Efficiency for a Perpendicular to Busbars Crack Which Effects 1, 2, 3 and 4 (1-8 busbars) PV Solar Cells

3.5. Multiple directions crack

Multiple directions cracks have the highest degradation in the PV measured output power. Three different measured data are presented in Fig. 8(A). As illustrated in Fig. 8(B), multiple directions crack effects 5 solar cells reduce the power efficiency of the PV module up to 8.42%. However, the average reduction in the power for a multiple directions crack effects 1 solar cell with an approximate broken area less than 46.2 mm^2 is equal to 1.04%.

Table VII shows a brief explanation for the T-test values and whether a multiple directions crack has a significant or not significant impact on the total output power produced by a cracked PV module.
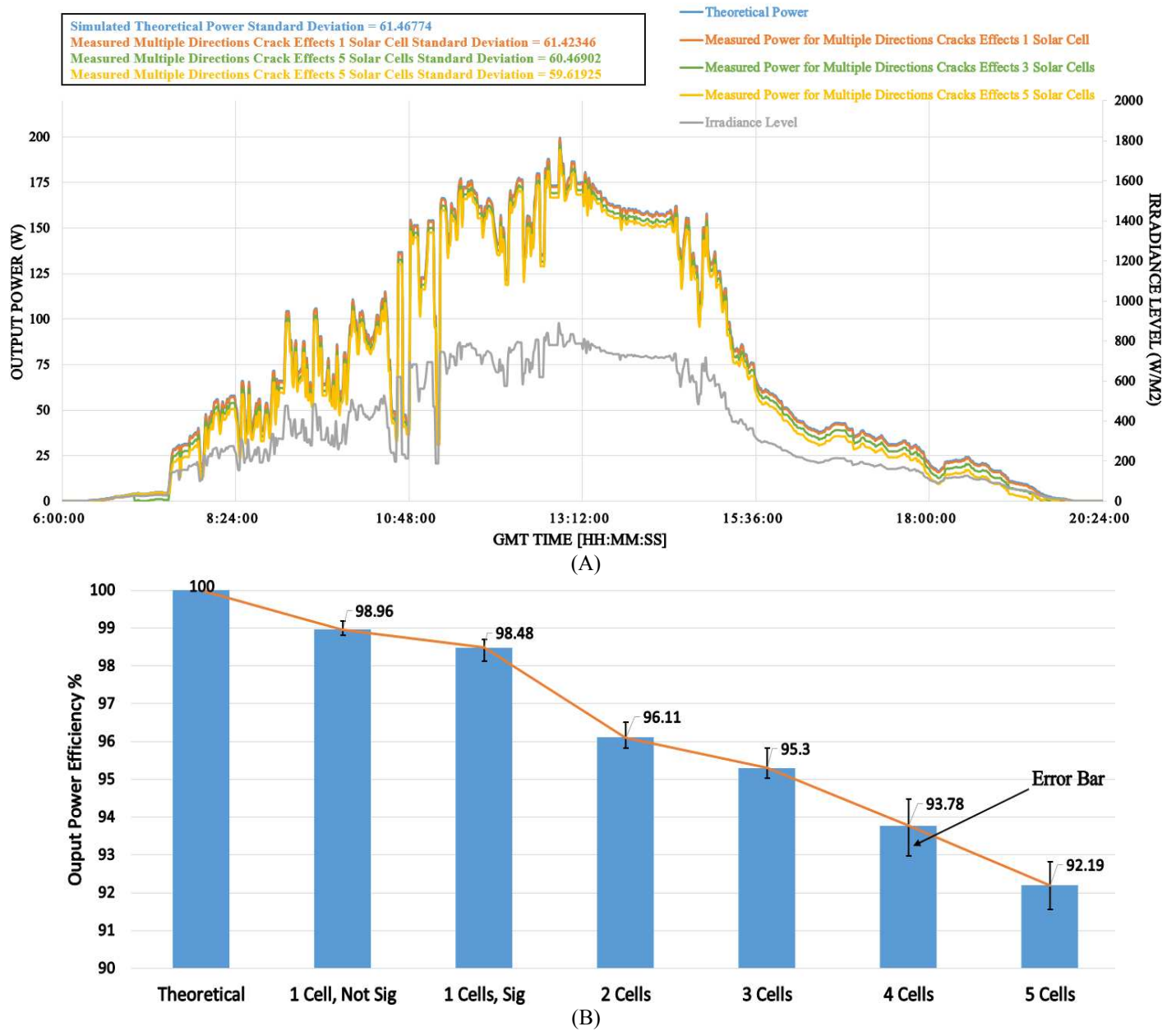
Fig. 8.   (A) Real-Time Long-Term Measured Data for a Multiple Directions Crack Effects on 1, 3 and 5 Solar Cells; (B) Output Power Efficiency for a Multiple Directions Crack Which Effects 1,2,3,4 and 5 PV Solar Cells

Table VII

Multiple Directions Cracks Performance Indicators

	Number of Effected Solar Cells	Approximate Area Broken (mm)	T-test Value	Significant/Not Significant Effect on the PV Power Performance	Fitted Line Regression Equation
Multiple Directions Crack	1	$1\ mm^2 - 45\ mm^2$	$2.06 - 2.44$	**Not Significant**	$P_{TH} = 0.3679 + 1.004\ P_{Meas}$
		$46.2\ mm^2 - 1000\ mm^2$	$2.68 - 2.88$	Significant	$P_{TH} = 0.5330 + 1.005\ P_{Meas}$
	2	$100\ mm^2 - 3700\ mm^2$	$3.25 - 3.33$	Significant	$P_{TH} = 1.028 + 1.012\ P_{Meas}$
	3	$170\ mm^2 - 5000\ mm^2$	$4.70 - 4.88$	Significant	$P_{TH} = 1.554 + 1.019\ P_{Meas}$
	4	$223\ mm^2 - 8200\ mm^2$	$6.17 - 6.31$	Significant	$P_{TH} = 2.015 + 1.027\ P_{Meas}$
	5	$400\ mm^2 - 9800\ mm^2$	$7.30 - 7.52$	Significant	$P_{TH} = 2.577 + 1.033\ P_{Meas}$

4. Discussion

4.1. Overall cracks assessment

The observed modules have 38 PV modules with various crack-types. The probability of occurrence for each crack type can be seen in Fig. 4. Before considering the statistical approach, it is hypothetically true to say that 84.4% has a significant impact on the output power performance. However, the statistical approach has confirmed that this is incorrect, because only 60% has a significant impact on the output power performance for all examined PV modules.

This result can be investigated further more by applying the same statistical approach on various PV systems in different regions around the world. The only difference might be the confidence interval limitations (99%, 95% and 90%) due to the various accuracy rates for the instrumentation used in the PV systems such as the Voltage sensors, Current sensors and Temperature sensors.

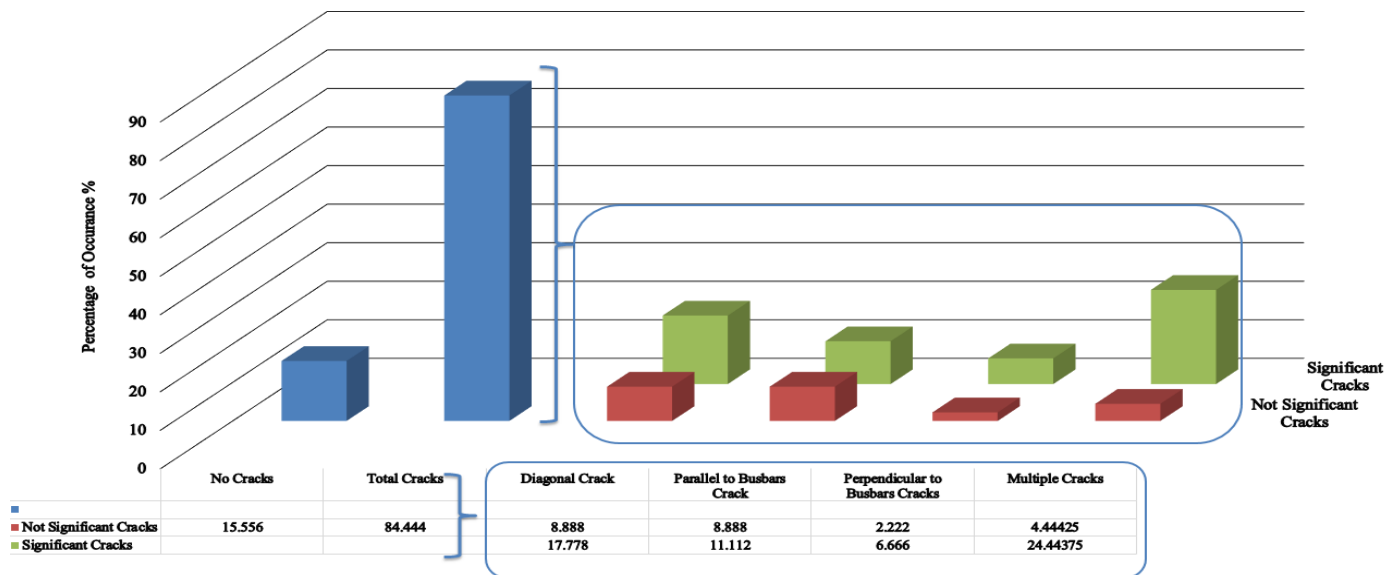|	No Cracks	Total Cracks	Diagonal Crack	Parallel to Busbars Crack	Perpendicular to Busbars Cracks	Multiple Cracks
Not Significant Cracks	15.556	84.444	8.888	8.888	2.222	4.44425
Significant Cracks			17.778	11.112	6.666	24.44375

Fig. 19.   Percentage of Cracks in the Examined PV modules, overall significant Cracks equals to 60% out of 84.444%

4.2 Surface damage

For better understanding how some cracks effects the surface of the PV modules, we have created a MATLAB code which can simulate the measured data of a cracked PV module in order to evaluate the surface shape for a particular crack-type using Surf(x, y, z) MATLAB function [24].

Fig. 10(A) shows a diagonal crack ($+45^0$) effects 3 solar cells. It is clear that the surface of three different solar cells are damaged (Noted as 1, 2 and 3). The degradation of the power for the solar cells is between 0.5 and 1 Watt. Overall PV module efficiency can be estimated by the MATLAB code which is equal to 98.61%, this result can be illustrated in Figs. 5(B) and 10(A).

Similarly, Fig 10(B) describes the surface shape of a parallel to busbars crack which effects 3 solar cells. The degradation of the power in the affected solar cells is between 2.5 and 2 Watt. The

261 overall power efficiency of the PV module is equal to 97.41% which is very similar to the value
262 (97.4%) described earlier in Fig. 6(B).

263 The surface shape for a perpendicular to busbars crack effects 3 solar cells, 6 Busbars is illustrated
264 in Fig. 10(C). However, Fig. 10(D) shows a cracked surface for a PV module that is affected by a
265 multiple directions crack on 3 different solar cells. Moreover, a perpendicular crack effects a solar
266 cell with 2 busbars has an estimated degradation of power equals to 1.5 Watt. Overall efficiency
267 of the cracked surfaces is equal to 97.28% for a perpendicular to busbars crack which effects 3
268 solar cells (6 busbars), and 95.3% for a multiple directions crack which effects 3 solar cells.
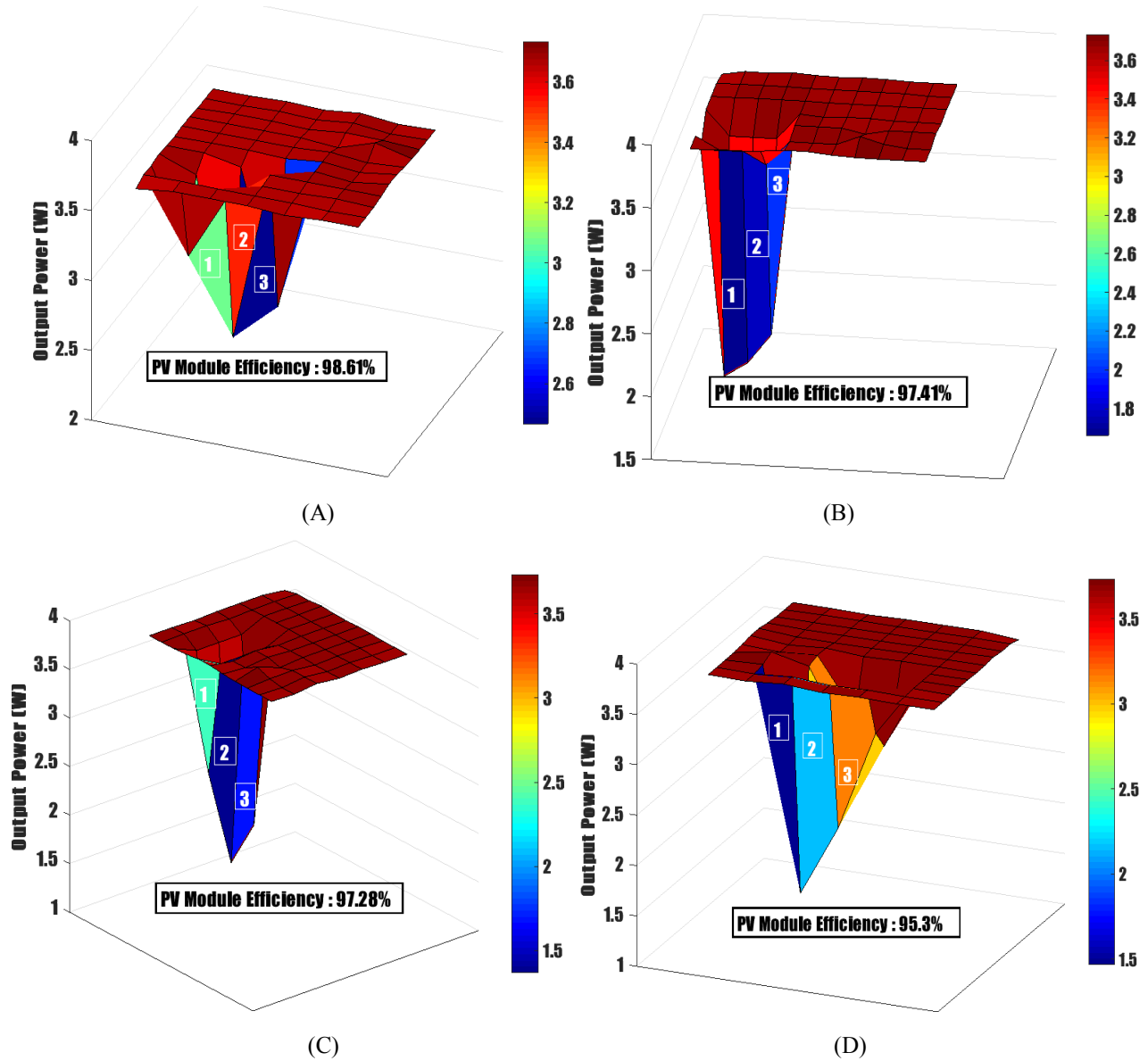

Fig. 10. (A) Surface Shape for a Diagonal (+45⁰) Crack Effects 3 Solar Cells; (B) Surface Shape for a Parallel to Busbars Crack Effects 3 Solar Cells (C) Surface Shape for a Perpendicular to Busbars Crack Effects 3 Solar Cells, 6 Busbars; (D) Surface Shape for a Multiple Directions Crack Effects 3 Solar Cells

16

5. Conclusion

This paper propose a new statistical algorithm to identify the significant of the cracks on the output power performance of the PV modules. The algorithm is developed using a Virtual Instrumentation (VI) LabVIEW software. We have examined 45 PV modules with various crack-type such as diagonal, parallel to busbars, perpendicular to busbars and multiple directions crack.

Before considering the statistical approach, 84.44% of the examined PV modules have a significant impact on the output power performance. However, the statistical approach has confirmed that this result is incorrect, since only 60% of the examine PV cracks have a significant impact on the output power performance.

Based on the measured output power data of each crack-type PV module, we have evaluated the fitted line regression equations. Subsequently, the surface of cracked PV modules have been demonstrated using Surf(x, y, z) MATLAB Function.

For further work, we are designing a generic algorithm based on statically analysis techniques to detect multiple faults in PV systems such as DC-Side faults, AC-Side faults, PV cracks and shading effect.

6. Acknowledgment

References

[1] Rajput, P., Tiwari, G. N., Sastry, O. S., Bora, B., & Sharma, V. (2016). Degradation of mono-crystalline photovoltaic modules after 22years of outdoor exposure in the composite climate of India. *Solar Energy*, *135*, 786-795.

[2] Dhimish, M., Holmes, V., & Dales, M. (2016, September). Grid-connected PV virtual instrument system (GCPV-VIS) for detecting photovoltaic failure. In *Environment Friendly Energies and Applications (EFEA), 2016 4th International Symposium on* (pp. 1-6). IEEE.

[3] Sharma, V., & Chandel, S. S. (2013). Performance and degradation analysis for long term reliability of solar photovoltaic systems: a review. *Renewable and Sustainable Energy Reviews*, *27*, 753-767.

[4] Köntges, M., Kunze, I., Kajari-Schröder, S., Breitenmoser, X., & Bjørneklett, B. (2010, September). Quantifying the risk of power loss in PV modules due to micro cracks. In *25th European Photovoltaic Solar Energy Conference, Valencia, Spain* (pp. 3745-3752).

[5] Kajari-Schröder, S., Kunze, I., Eitner, U., & Köntges, M. (2011). Spatial and orientational distribution of cracks in crystalline photovoltaic modules generated by mechanical load tests. *Solar Energy Materials and Solar Cells*,*95*(11), 3054-3059.

303 [6] Dallas, W., Polupan, O., & Ostapenko, S. (2007). Resonance ultrasonic vibrations for crack
304 detection in photovoltaic silicon wafers. *Measurement Science and Technology*, *18*(3), 852.

305 [7] Morlier, A., Haase, F., & Köntges, M. (2015). Impact of cracks in multicrystalline silicon solar
306 cells on PV module power—A simulation study based on field data. *IEEE Journal of*
307 *Photovoltaics*, *5*(6), 1735-1741.

308 [8] Paggi, M., Corrado, M., & Rodriguez, M. A. (2013). A multi-physics and multi-scale numerical
309 approach to microcracking and power-loss in photovoltaic modules. *Composite Structures*, *95*,
310 630-638.

311 [9] Köntges, M., Kajari-Schröder, S., Kunze, I., & Jahn, U. (2011, September). Crack statistic of
312 crystalline silicon photovoltaic modules. In *26th European Photovoltaic Solar Energy Conference*
313 *and Exhibition* (pp. 5-6).

314 [10] van Mölken, J. I., Yusufoğlu, U. A., Safiei, A., Windgassen, H., Khandelwal, R., Pletzer, T.
315 M., & Kurz, H. (2012). Impact of micro-cracks on the degradation of solar cell performance based
316 on two-diode model parameters.*Energy Procedia*, *27*, 167-172.

317 [11] Kaplani, E. (2016, April). Degradation in Field-aged Crystalline Silicon Photovoltaic
318 Modules and Diagnosis using Electroluminescence Imaging. In*Presented at 8th International*
319 *Workshop on Teaching in Photovoltaics (IWTPV'16)* (Vol. 7, p. 8).

320 [12] Munoz, M. A., Alonso-Garcia, M. C., Vela, N., & Chenlo, F. (2011). Early degradation of
321 silicon PV modules and guaranty conditions. *Solar energy*,*85*(9), 2264-2274.

322 [13] Gerber, A., Huhn, V., Tran, T. M. H., Siegloch, M., Augarten, Y., Pieters, B. E., & Rau, U.
323 (2015). Advanced large area characterization of thin-film solar modules by electroluminescence
324 and thermography imaging techniques.*Solar Energy Materials and Solar Cells*, *135*, 35-42.

325 [14] Köntges, M., Siebert, M., Hinken, D., Eitner, U., Bothe, K., & Potthof, T. (2009, September).
326 Quantitative analysis of PV-modules by electroluminescence images for quality control. In *24th*
327 *European Photovoltaic Solar Energy Conference, Hamburg, Germany* (pp. 21-24).

328 [15] Berardone, I., Corrado, M., & Paggi, M. (2014). A generalized electric model for mono and
329 polycrystalline silicon in the presence of cracks and random defects. *Energy Procedia*, *55*, 22-29.

330 [16] Spataru, S., Hacke, P., Sera, D., Glick, S., Kerekes, T., & Teodorescu, R. (2015, June).
331 Quantifying solar cell cracks in photovoltaic modules by electroluminescence imaging.
332 In *Photovoltaic Specialist Conference (PVSC), 2015 IEEE 42nd* (pp. 1-6). IEEE.

333 [17] Dhimish, M., Holmes, V., & Dales, M. (2016, September). Grid-connected PV virtual
334 instrument system (GCPV-VIS) for detecting photovoltaic failure. In *Environment Friendly*
335 *Energies and Applications (EFEA), 2016 4th International Symposium on* (pp. 1-6). IEEE.

336 [18] Dhimish, M., & Holmes, V. (2016). Fault detection algorithm for grid-connected photovoltaic
337 plants. *Solar Energy*, *137*, 236-245.

338 [19] Silvestre, S., Chouder, A., & Karatepe, E. (2013). Automatic fault detection in grid connected
339 PV systems. *Solar Energy*, *94*, 119-127.

340 [20] Kajari-Schröder, S., Kunze, I., Eitner, U., & Köntges, M. (2011). Spatial and orientational
341 distribution of cracks in crystalline photovoltaic modules generated by mechanical load tests. *Solar*
342 *Energy Materials and Solar Cells*,*95*(11), 3054-3059.

343 [21] McEvoy, A., Castaner, L., Markvart, T., 2012. Solar Cells: Materials, Manufacture and

344 Operation. Academic Press.

345 [22] Miller, J. N., & Miller, J. C. (2010; 2011). Statistics and chemometrics for analytical
346 chemistry (6th ed.). Harlow: Prentice Hall.

347 [23] Köntges, M., Kajari-Schröder, S., & Kunze, I. (2013). Crack statistic for wafer-based silicon
348 solar cell modules in the field measured by UV fluorescence. *IEEE Journal of Photovoltaics*, *3*(1),
349 95-101.

350 [24] Guo, G., Luc, S., Marco, E., Lin, T. W., Peng, C., Kerenyi, M. A., ... & Neff, T. (2013).
351 Mapping cellular hierarchy by single-cell analysis of the cell surface repertoire. *Cell stem*
352 *cell*, *13*(4), 492-505.